



Pre-operative Prediction of Ki-67 Expression in Various Histological Subtypes of Lung Adenocarcinoma Based on CT Radiomic Features

Zhiwei Huang^{1,2†}, Mo Lyu^{2,3†}, Zhu Ai^{2†}, Yirong Chen^{1,2}, Yuying Liang² and Zhiming Xiang^{2*}

OPEN ACCESS

Edited by:

Kee Yuan Ngiam,
National University Health
System, Singapore

Reviewed by:

Zhang Wang,
South China Normal University, China
Jinglei Li,
Guangdong Provincial People's
Hospital, China
Kai Wu,
South China University of Technology,
China

*Correspondence:

Zhiming Xiang
xiangzhiming@pyhospital.com.cn

†These authors have contributed
equally to this work and share first
authorship

Specialty section:

This article was submitted to
Surgical Oncology,
a section of the journal
Frontiers in Surgery

Received: 05 July 2021

Accepted: 09 September 2021

Published: 18 October 2021

Citation:

Huang Z, Lyu M, Ai Z, Chen Y, Liang Y
and Xiang Z (2021) Pre-operative
Prediction of Ki-67 Expression in
Various Histological Subtypes of Lung
Adenocarcinoma Based on CT
Radiomic Features.
Front. Surg. 8:736737.
doi: 10.3389/fsurg.2021.736737

¹ Graduate School, Guangzhou University of Chinese Medicine, Guangzhou, China, ² Department of Radiology, Guangzhou Panyu Central Hospital, Guangzhou, China, ³ School of Life Sciences, South China Normal University, Guangzhou, China

Purpose: The aims of this study were to combine CT images with Ki-67 expression to distinguish various subtypes of lung adenocarcinoma and to pre-operatively predict the Ki-67 expression level based on CT radiomic features.

Methods: Data from 215 patients with 237 pathologically proven lung adenocarcinoma lesions who underwent CT and immunohistochemical Ki-67 from January 2019 to April 2021 were retrospectively analyzed. The receiver operating curve (ROC) identified the Ki-67 cut-off value for differentiating subtypes of lung adenocarcinoma. A chi-square test or *t*-test analyzed the differences in the CT images between the negative expression group ($n = 132$) and the positive expression group ($n = 105$), and then the risk factors affecting the expression level of Ki-67 were evaluated. Patients were randomly divided into a training dataset ($n = 165$) and a validation dataset ($n = 72$) in a ratio of 7:3. A total of 1,316 quantitative radiomic features were extracted from the Analysis Kinetics (A.K.) software. Radiomic feature selection and radiomic classifier were generated through a least absolute shrinkage and selection operator (LASSO) regression and logistic regression analysis model. The predictive capacity of the radiomic classifiers for the Ki-67 levels was investigated through the ROC curves in the training and testing groups.

Results: The cut-off value of the Ki-67 to distinguish subtypes of lung adenocarcinoma was 5%. A comparison of clinical data and imaging features between the two groups showed that histopathological subtypes and air bronchograms could be used as risk factors to evaluate the expression of Ki-67 in lung adenocarcinoma ($p = 0.005$, $p = 0.045$, respectively). Through radiomic feature selection, eight top-class features constructed the radiomic model to pre-operatively predict the expression of Ki-67, and the area under the ROC curves of the training group and the testing group were 0.871 and 0.8, respectively.

Conclusion: Ki-67 expression level with a cut-off value of 5% could be used to differentiate non-invasive lung adenocarcinomas from invasive lung adenocarcinomas. It is feasible and reliable to pre-operatively predict the expression level of Ki-67 in lung

adenocarcinomas based on CT radiomic features, as a non-invasive biomarker to predict the degree of malignant invasion of lung adenocarcinoma, and to evaluate the prognosis of the tumor.

Keywords: lung adenocarcinoma, Ki-67, computed tomography, radiomics, pre-operative prediction, non-invasive biomarker

INTRODUCTION

Lung adenocarcinoma is the most commonly diagnosed histological subtype of non-small-cell lung cancer (NSCLC), which is the leading cause of cancer-related deaths worldwide (1). In 2011, a new classification system for lung adenocarcinomas according to the International Association for the study of Lung Cancer (IASLC), American Thoracic Society (ATS), and European Respiratory Society (ERS) has been put forward, wherein the lung adenocarcinomas are mainly classified as atypical adenomatous hyperplasia (AAH), adenocarcinoma *in situ* (AIS), minimally invasive adenocarcinoma (MIA), and invasive adenocarcinoma (IAC). Among them, AAH and AIS were pre-invasive lesions (2). More and more treatment methods can be used for the treatment of lung cancer. However, many patients, even patients with resectable lung cancer, still have poor prognoses (3). For lung adenocarcinoma, studies have found that, even for patients with complete surgical resection and in pathologic stage T1 (pathologic-T1, pT1), the treatment effects and prognoses may be significantly different (4). There is an urgent need to determine reliable prognostic factors that can predict clinical outcomes and more precisely stratify the group of patients susceptible to poorer outcomes.

Currently, Ki-67 is commonly regarded as a prognosis biomarker to predict the cell proliferation and aggressiveness of tumors in clinical practice, which can be used for quantitative analysis of tumor growth fraction and the classification of tumors and for assisting in early diagnosis and therapeutic effect evaluations (5). Ki-67 is expressed at all stages of the cell cycle except G₀, with the highest expression levels in the G₂/M phase. It has been reported that the overall survival (OS) and disease-free survival (DFS) of patients with high Ki-67 expression are shorter than those with low Ki-67 expression (5–7). Previous studies have identified the Ki-67 labeling index as a strong prognostic biomarker for lung adenocarcinoma (8, 9). Yamashita et al. found that Ki-67 can be used as an indicator of recurrence of lung cancer after resection (10), and the level of its positive expression is closely related to the differentiation degree, lymph node metastasis, and other factors of lung cancer (8, 11). The most commonly used method to quantify Ki-67 expression is immunohistochemistry (IHC), which is not practical for the dynamic monitoring of Ki-67 during lung cancer treatment because of invasion, which is time-consuming (12). Due to the existence of tumor heterogeneity, Ki-67 values varied in different regions of the tumor samples, and traditional invasive immunohistochemical methods only evaluate the biopsy specimens of a small sample of the tissue and cannot reflect the overall heterogeneity of the tumor (13, 14). Therefore, finding a non-invasive, cost-effective, and comprehensive

method for clinical Ki-67 expression level assessment is necessary.

Radiomics is a recently emerging technique in computational medical imaging. It involves the extraction and analyses of a large number of quantitative imaging features from medical images (15, 16). It is different from traditional methods because it converts medical images into mineable high-dimensional data. Radiomics can help support patient diagnosis, prognosis, treatment, and prediction in clinical practice. The relationship between Ki-67 expression level and radiomic features has always been a hot topic. Studies have shown that radiomics can be used to pre-operatively predict the expression level of Ki-67 in breast cancer (17) and adrenal cancer (18). In addition, several studies have shown that the quantitative imaging features from CT can predict Ki-67 levels and subtypes in patients with lung cancer (19, 20), but the role of Ki-67 in distinguishing the pathological stages of lung adenocarcinoma remains unclear (12, 21). To our knowledge, there have been no studies on the use of CT-based radiomic features to predict Ki-67 expression levels in subtypes of lung adenocarcinoma.

This study aimed to investigate the correlation between Ki-67 expression level and the subtypes of lung adenocarcinoma and to assess whether CT-based radiomic features could serve as non-invasive predictors of the Ki-67 levels in patients with lung adenocarcinoma.

MATERIALS AND METHODS

Patient Characteristics

We retrospectively collected data from patients who underwent a chest CT scan, Ki-67 expression level detection, and post-operative pathological confirmation of lung adenocarcinoma at our institute from January 2019 to April 2021. The inclusion criteria were: (1) patients confirmed with lung adenocarcinoma by surgical resection, (2) maximum diameter of tumor ≤ 3 cm, (3) complete clinicopathological data, (4) IHC examination of Ki-67 expression levels, and (5) complete CT images. The exclusion criteria were: (1) greatest tumor diameter > 3 cm, (2) radiotherapy, chemotherapy, or radiotherapy and chemotherapy were performed before surgery, and (3) incomplete or poor-quality CT images. Our institutional review board approved this retrospective study, and the requirement for informed consent was waived.

Computed Tomography Examination

All patients in this study used a 64-slice CT scanner (Discovery CT 750 HD, GE Healthcare, Chicago, IL, USA) for their chest scans. All CT scans were obtained with the patients in the supine position and holding their breath at the end of a full inspiration.

The scan ranged from above the apex of the lungs to below the level of the diaphragm. The scanning parameters were as follows: tube voltage of 120 or 140 kV, tube current of 200–340 mA, beam pitch of 1.2, pixel resolution of 512×512 , field of view (FOV) of 360 mm, thickness of 5 mm, and reconstructed slice thickness and slice increment of 1 mm. Afterward, the CT scans were reviewed as lung window images (window width = 1,200 HU; window level = -700 HU) and mediastinal window images (window width = 350 HU; window level = 50 HU). All images were exported in a DICOM format for image feature extraction after scanning.

The CT imaging signs included (22): (1) lesion location, (2) maximum diameter of the tumor on axial images, (3) tumor-lung interface: clear or unclear, (4) density: pure ground-glass opacity, mixed ground-glass opacity, and solid nodule, (5) spiculation, (6) lobulation, (7) bubble-like lucency, (8) air bronchogram sign, (9) vascular sign, and (10) pleural traction. Two diagnostic radiologists with 3 and 9 years of experience reviewed the CT images of each patient and identified positive and negative findings by consensus. The entire process was performed without the patient having knowledge of the pathological results.

Immunohistochemical Analysis

Lung tissues were fixed with a 10% buffered formaldehyde solution by transbronchial or transpleural perfusion for ~ 48 h and embedded in paraffin wax. Tissue sections were stained with HE. A mouse anti-human Ki-67 monoclonal antibody (Beijing Zhongshan Jinqiao Biotechnology Co., Ltd., Beijing, China) was used to perform the immunohistochemical detection according to the kit instructions. Positive and negative controls were set up, respectively. Ki-67 was positive with brown-yellow granules in the nucleus. The number of Ki-67 positive tumor cells was calculated in five fields of high-power field ($\times 400$) under light microscopes. The percentage of Ki-67 expression level positive staining of tumor cells in each field = the number of positive tumor cells in each field/total tumor cells in each field $\times 100\%$. The Ki-67 indices in five fields were calculated and averaged. Histological and cytological subtypes were assessed according to the WHO classification system for lung cancer (5th version) (23). The thresholding of the Ki-67 expression level was used to separate the tumor samples into positive and negative groups: The expression level of Ki-67 $\leq 5\%$ was negative, and $> 5\%$ was positive (24).

Radiomics Analysis

Image Pre-processing and Image Segmentation

Firstly, the CT scan images of all patients were exported in a DICOM format from the PACS system workstations, and the AK (Analysis Kinetics, V3.2.0, Workbench2014, GE Healthcare) software was used to preprocess the resampled images of $0.5 \times 0.5 \times 0.5$ on the X, Y, and Z axes, respectively. The three-dimensional segmentation of the tumor regions of interest (ROIs) was performed using the ITK-SNAP software (version 3.8, Philadelphia, PA, USA) with the window width and window level as 1,200 HU and -700 HU, respectively. Then, the ROIs were outlined, and the outlined image was saved in the format of

“Merge. nii.” The scope of the image delineation includes tumor necrosis, cystic, and cavity, excluding burr, thickened pleura, and surrounding signs. The continuous delineation includes the whole lesion. If it is found to be contradictory, other senior radiologists will evaluate the tumor mask again to reach an agreement.

Radiomic Feature Extraction

The data were imported into the AK (V3.2.0, Workbench2014, GE Healthcare) analysis software to extract radiomic features, including features of first order, shape (Shape), gray-level co-occurrence matrix (GLCM), gray-level run-length matrix (GLRLM), gray-level size-zone matrix (GLSZM), gray-level dependence matrix (GLDM), and features of neighborhood gray difference matrix (NGTDM). The selected image transformations were: logarithmic transformation (LoG), parameter Sigma selection 2.0, 3.0; wavelet transformation (Wavelet), Level 1; local binary mode (LBP), Level 2, Radius 1.0, Subdivision select 1. A total of 1,316 features were extracted.

Radiomic Feature Selection and Classifier Construction

The interobserver intraclass correlation coefficient (ICC) selects values > 0.75 . Stratified sampling was used to divide all the patients into a training cohort ($n = 165$) and a validation cohort ($n = 72$) according to a ratio of 7:3. First, an ANOVA was performed to remove features with $p > 0.05$, and then the rest of the radiomic features were retained to select the most relevant features using recursive feature elimination (RFE). Next, the least absolute shrinkage and selection operator (LASSO) model, which could improve prediction accuracy and interpretation, was used to further select the features. According to Mann–Whitney U test, the top-class features were screened out to build the final logistic regression classifier, which was used to perform radiomic feature selection in the training dataset. Classification performance was evaluated using the area under the receiver operating characteristic curve (AUC). Finally, a radiomic score (Rad score) was developed using the logistic regression model and then used to calculate the training and validation datasets. A simplified flowchart of the study is given in **Figure 1**.

Statistical Analysis

Clinicopathologic Characteristics of Patients

All statistical analyses were performed with SPSS version 21.0 (IBM Corporation, Armonk, NY, USA). Results were given as mean \pm SD or median and range values. The chi-square test or Fisher’s exact test was adopted to compare the distribution of the categorical variables. Student’s t -test or one-way ANOVA was also calculated for the comparison of continuous variables. Mann–Whitney U testing was used for non-parametric data. Binary logistic regression was used to analyze the potential risk factors affecting the Ki-67 expression level. The cut-off value of the labeling index was obtained from the receiver operating curve (ROC) with the Youden index. The statistical analysis was considered significant when the p -value was < 0.05 .

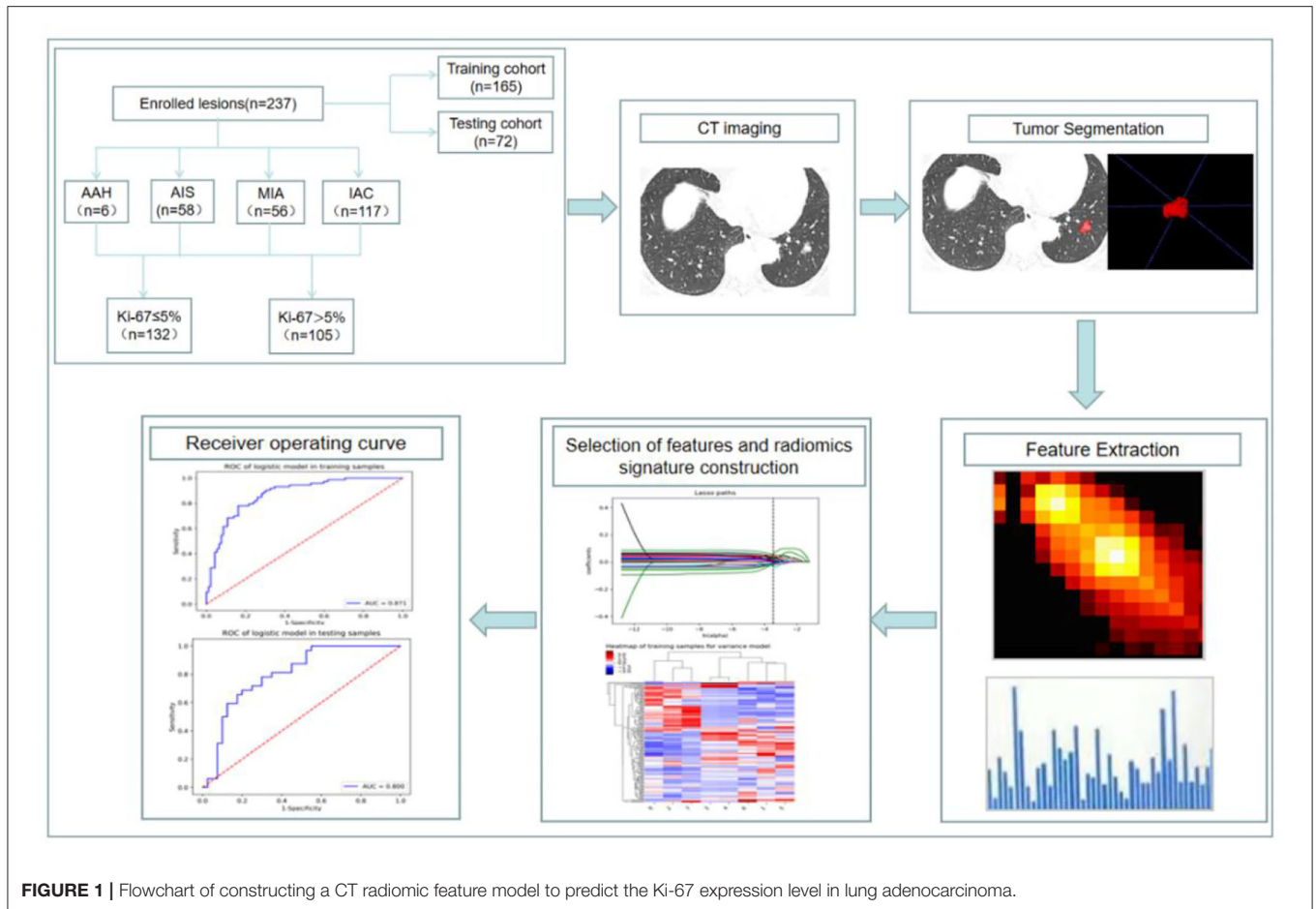


FIGURE 1 | Flowchart of constructing a CT radiomic feature model to predict the Ki-67 expression level in lung adenocarcinoma.

Performance of the Radiomic Prediction Model

To evaluate the performance of the proposed radiomic prediction model, we adopted accuracy, sensitivity, specificity, positive predictive value, and negative predictive value as the evaluation indexes. Furthermore, the ROC curves and the AUCs were calculated to quantitatively assess the predictive capacity of the radiomic classifiers in the training and validation datasets. A *p*-value of <math><0.05</math> was considered statistically significant.

RESULTS

Characteristics of Study Subjects

The clinicopathologic characteristics of the patients with lung adenocarcinoma were summarized in **Table 1**. After screening, a total of 215 patients met the requirements. Among them, 19 patients had multiple lesions. There were 68 males (31.63%) and 147 females (68.37%) with a median age of 56 years old. One hundred ninety-six patients (91.16%) were non-smokers. Seventeen patients (7.91%) had a history of non-pulmonary tumors, 9 had thyroid cancer, 4 had breast cancer, 1 had cervical cancer, 1 had endometrial squamous cell carcinoma, 1 had colon cancer, and 1 had vocal cord squamous cell carcinoma. In the end, 237 lung adenocarcinoma lesions were selected for our study.

TABLE 1 | Patient characteristics on a per patient level.

| Variables | n (%) or Median (range) |
|-------------------------------------|-------------------------|
| Age (years) | 56.00 (22,82) |
| Gender | |
| Female | 147 (68.37) |
| Male | 68 (31.63) |
| Smoking history | |
| Never | 196 (91.16) |
| Ever | 19 (8.84) |
| History of malignancies | 17 (7.91) |
| Breast cancer | 4 (1.86) |
| Cervical cancer | 1 (0.47) |
| Thyroid cancer | 9 (4.19) |
| Colon cancer | 1 (0.47) |
| Endometrial squamous cell carcinoma | 1 (0.47) |
| Vocal cord squamous cell carcinoma | 1 (0.47) |

Ki-67 Expression Levels and Histological Subtypes

As shown in **Tables 2, 3**, and **Figures 2A–C**, the pathological diagnoses based on multidisciplinary lung adenocarcinoma

TABLE 2 | The expression level of Ki-67 in various pathological subtypes of lung adenocarcinoma.

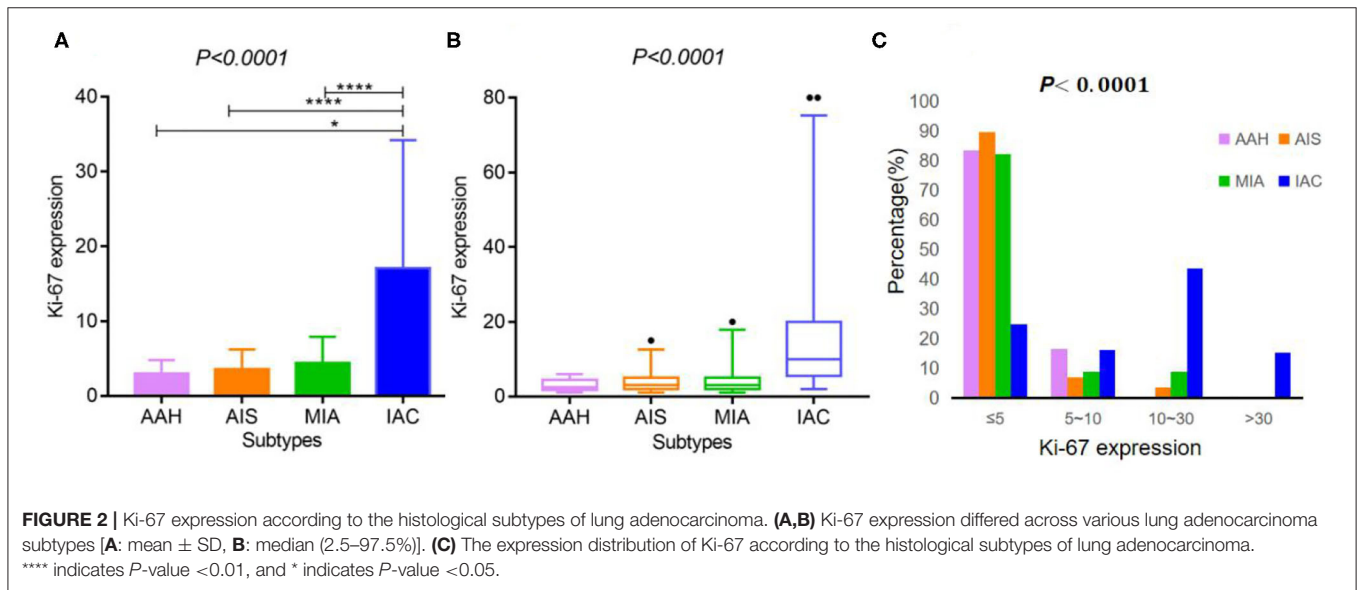
| Variables | AAH (n = 6) | AIS (n = 58) | MIA (n = 56) | Non-invasive adenocarcinoma (AAH/AIS/MIA) (n = 120) | IAC (n = 117) | P |
|-----------------------------|-------------|--------------|--------------|---|---------------|--------|
| Ki-67 expression (%) | | | | | | |
| mean ± SD | 3.00 ± 1.79 | 3.57 ± 2.63 | 4.39 ± 3.53 | 3.93 ± 3.07 | 17.09 ± 17.12 | <0.001 |
| Median (range) | 2.5 (1,6) | 3 (1,15) | 3 (1,20) | 3 (1,20) | 10 (2,80) | <0.001 |
| Ki-67 Subgroups (%) | | | | | | |
| ≤5 | 5 (83.33) | 52 (89.65) | 46 (82.14) | 103 (85.83) | 29 (24.79) | <0.001 |
| 5–10 | 1 (16.67) | 4 (6.90) | 5 (8.93) | 10 (8.34) | 19 (16.24) | |
| 10–30 | 0 | 2 (3.45) | 5 (8.93) | 7 (5.83) | 51 (43.59) | |
| >30 | 0 | 0 | 0 | 0 | 18 (15.38) | |

SD, standard deviation.

TABLE 3 | Area under the ROC curve (AUC) of the Ki-67 expression level among different pathological subtypes paired groups.

| Pairs | P | AUC | Optional cut-off value | Standard deviation | Asymptotic P-value | Asymptotic 95% Confidence interval | |
|---------------------|--------|-------|------------------------|--------------------|--------------------|------------------------------------|-------------|
| | | | | | | Lower limit | Upper limit |
| MIA vs. IAC | <0.001 | 0.851 | 5.5 | 0.030 | <0.001 | 0.792 | 0.909 |
| AAH/AIS vs. MIA/IAC | <0.001 | 0.787 | 6.5 | 0.030 | <0.001 | 0.729 | 0.846 |
| AAH/AIS/MIA vs. IAC | <0.001 | 0.872 | 5.5 | 0.023 | <0.001 | 0.828 | 0.916 |

AAH, atypical adenomatous hyperplasia; AIS, adenocarcinoma in situ; MIA, minimally invasive adenocarcinoma; IAC, invasive adenocarcinoma.



criteria were as follows: 6 patients (2.53%) had AAH, 58 patients (24.47%) had AIS, 56 patients (23.63%) had MIA, and 117 (49.37%) had IAC. The AAH subtype had the lowest Ki-67 expression level (3 ± 1.79), followed by AIS (3.57 ± 2.63), MIA (4.39 ± 3.53), and IAC (17.09 ± 17.12). The samples were further divided into four subgroups according to Ki-67 expression: ≤ 5 , 5–10, 10–30, and $>30\%$. In total, the group with Ki-67 expression levels $\leq 5\%$ was composed of pre-cellular

(AAH/AIS) (57/64, 89.06%), minimally invasive (46/56, 82.14%), and invasive adenocarcinomas (29/117, 24.79%). The group with Ki-67 expression levels $>5\%$ consisted of pre-cellular (7/64, 10.94%), minimally invasive (10/56, 17.86%), and invasive adenocarcinomas (88/117, 75.21%). By a one-way ANOVA, Tamhane’s T2 test (with a Levene test for uneven variance between groups) compared the expression levels of Ki-67, and it was found that there was no significant difference between the

AAH group and AIS group ($p = 0.608$), the AAH group and MIA group ($p = 0.347$), and the AIS group and MIA group ($p = 0.159$), but the AAH group ($p < 0.001$), AIS group ($p < 0.001$), and MIA group ($p < 0.001$) were significantly different from the IAC group.

The Optimal Ki-67 Cut-Off Points Among Different Pathological Subtypes Paired Groups of Lung Adenocarcinoma

As shown in **Table 3** and **Figures 3A–C**, the ROC curve was used to analyze the sensitivity, specificity, and cut-off value of Ki-67 as a discriminant index for different pathological subtypes of lung adenocarcinoma. Non-invasive lung adenocarcinoma (AAH/AIS/MIA) vs. invasive lung adenocarcinoma (AUC = 0.872) had the highest sensitivity and specificity, followed by MIA vs. IAC (AUC = 0.851) and pre-cellular (AAH/AIS) vs. MIA/IAC (AUC = 0.787) ($p < 0.001$). According to the cut-off points of each pairing group, when the expression of Ki-67 was $\leq 5\%$, it was more inclined to AAH, AIS, or MIA, while more than 5% corresponded to IAC.

Comparison of CT Imaging Signs and Clinical Data of Lung Adenocarcinoma in Ki-67 Negative and Positive Expression Group

In our study, the median expression of Ki-67 was 5%. In addition, the lung adenocarcinomas were divided into a non-invasive adenocarcinoma group (AAH/AIS/MIA group) and an invasive adenocarcinoma group according to the prognosis of the lesions. Those classified as MIA were grouped with AAH/AIS due to its good prognosis. Therefore, 5% was selected as the cut-off value for grouping different stages of lung adenocarcinoma. Patients were divided into two groups: 132 (55.7%) patients had negative Ki-67 expression, and 105 (44.3%) patients exhibited positive

Ki-67 expression. We first explored whether the imaging signs and clinical data could distinguish between the Ki-67 negative expression group and the Ki-67 positive expression group. The results showed that CT imaging signs (maximum diameter, density, shape, lobulation, spiculation, air bronchogram, vascular sign, and pleural traction) could be used to discriminate between the two groups ($p < 0.001$). There was a higher percentage of lymph node metastasis in the Ki-67 positive expression group than in the Ki-67 negative expression group ($p < 0.001$) (**Table 4**). Air bronchogram and histopathological subtype had moderate predictive values, and the AUC values were 0.711 and 0.809, respectively (**Table 5**). The Ki-67 positive expression group was more inclined to have air bronchograms than the Ki-67 negative expression group. The histopathological subtype of the Ki-67 positive expression group was more likely to be IAC, while the Ki-67 negative expression group was more likely to be a pre-invasive lesion (AAH and AIS) or MIA (**Figure 4**).

Feature Selection

Patients were randomly divided into a training dataset ($n = 165$) and a validation dataset ($n = 72$) in a ratio of 7:3. At last, 1,316 radiomic features were extracted from the AK software. After the application of LASSO logistic algorithm, eight radiomic features were finally selected as the optimal radiomic feature subset based on the relationship between the classification accuracy and the number of features for the radiomic classifier. In **Table 6**, eight optimal radiomic features include 1 first order histogram feature, 2 GLCM, 3 GLRLM, and 2 GLDM. **Figure 5** shows the correlation between the top eight features, namely, `lbp-3D-k_glrml_LongRunHighGrayLevelEmphasis` ($p < 0.001$), `lbp-3D-k_glrml_ShortRunLowGrayLevelEmphasis` ($p < 0.001$), `log-sigma-3-0-mm-3D_gldm_GrayLevelVariance` ($p < 0.001$), `original_gldm_LowGrayLevelEmphasis` ($p < 0.001$), `original_glrml_LowGrayLevelRunEmphasis` ($p < 0.001$), `wavelet`

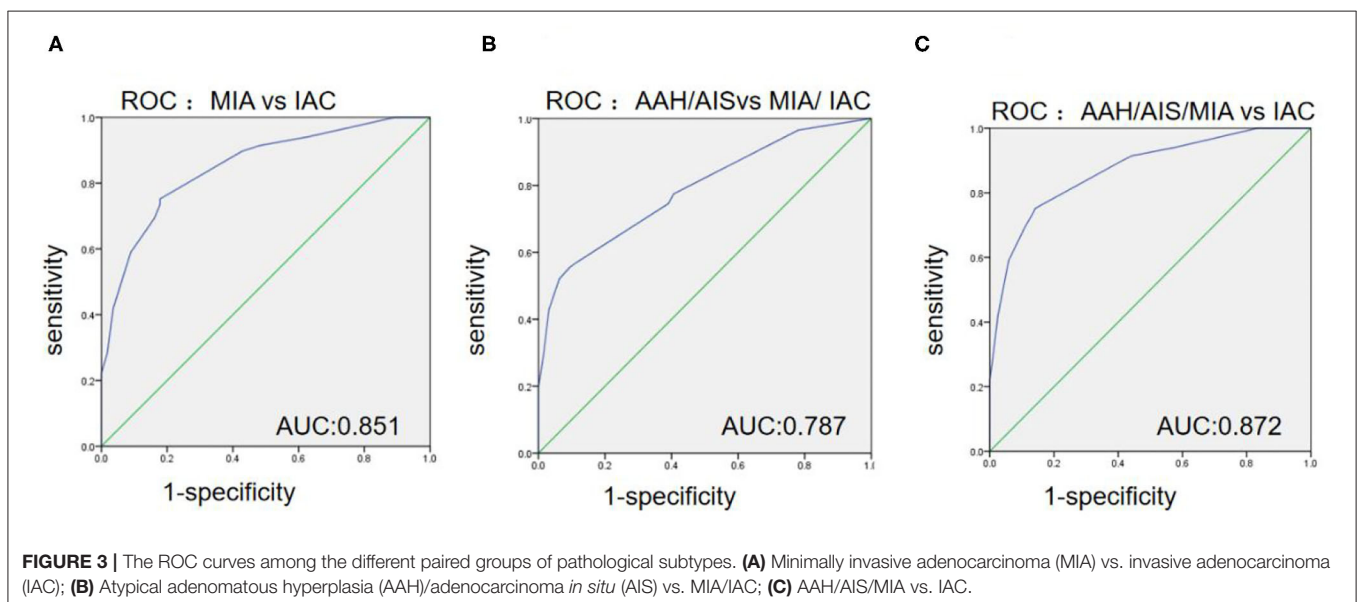


TABLE 4 | Comparison of imaging features and histopathological subtypes in the Ki-67 negative and positive expression groups of lung adenocarcinoma.

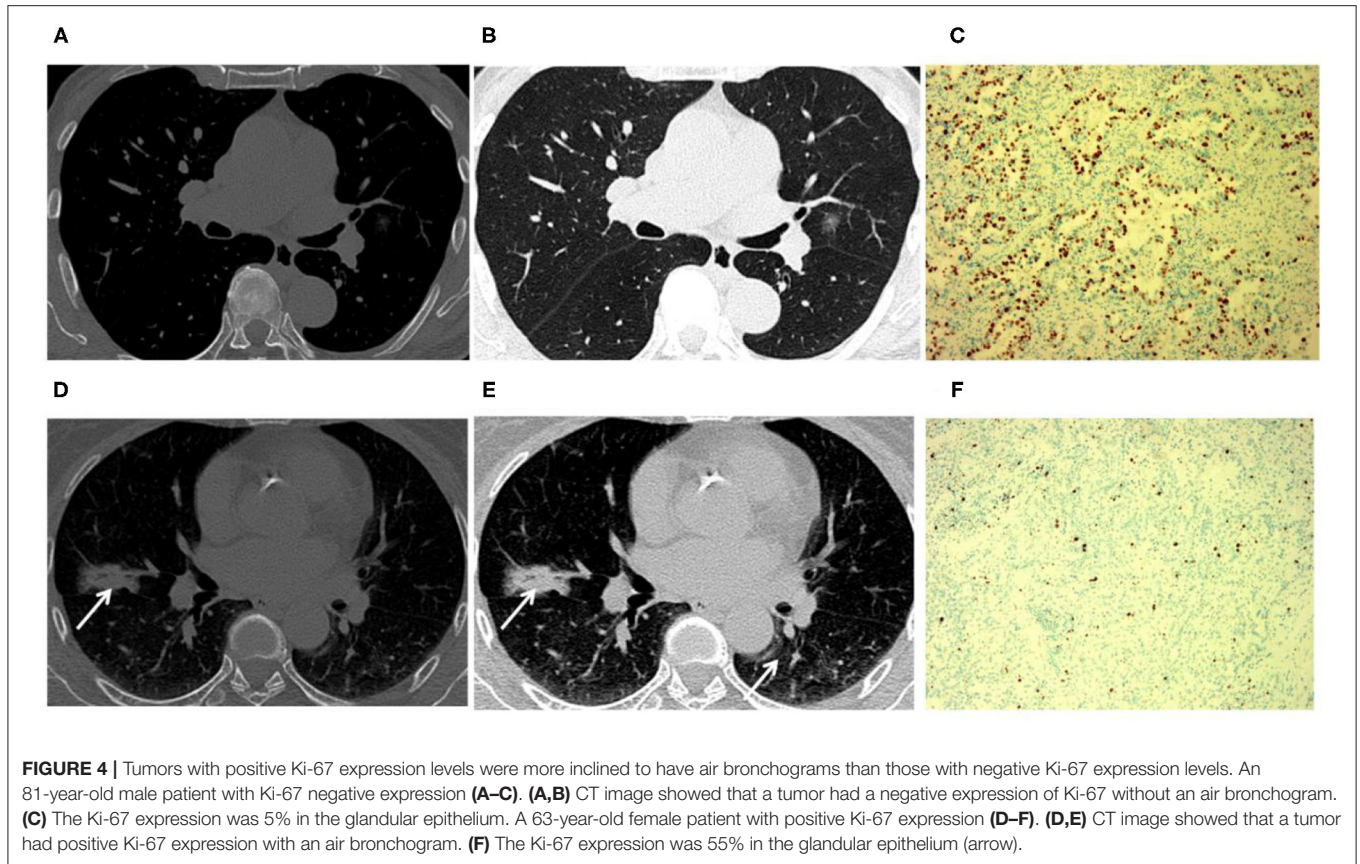
| Characteristics | Negative Ki-67 expression group (n = 132) | | Total | Positive Ki-67 expression group (n = 105) | | Total | p |
|------------------------------|---|-------------------------|--------------|---|-------------------------|--------------|--------|
| | Training cohort (n = 92) | Testing cohort (n = 40) | | Training cohort (n = 73) | Testing cohort (n = 32) | | |
| Pathological subtype | | | | | | | <0.001 |
| Pre-cellular (AAH/AIS) | 38 (28.79) | 19 (14.39) | 57 (43.18) | 4 (3.81) | 3 (2.86) | 7 (6.67) | |
| MIA | 35 (26.52) | 11 (8.33) | 46 (34.85) | 7 (6.67) | 3 (2.86) | 10 (9.52) | |
| IAC | 19 (14.39) | 10 (7.58) | 29 (21.97) | 62 (59.05) | 26 (24.76) | 88 (83.81) | |
| LPA | 1 (0.76) | 4 (3.03) | 5 (3.79) | 11 (10.48) | 1 (0.95) | 12 (11.43) | |
| APA | 15 (11.36) | 4 (3.03) | 19 (14.39) | 39 (37.14) | 19 (18.10) | 58 (55.24) | |
| PPA | 2 (1.52) | 1 (0.76) | 3 (2.27) | 7 (6.67) | 3 (2.86) | 10 (9.52) | |
| MPA | 0 | 0 | 0 | 2 (1.90) | 1 (0.95) | 3 (2.86) | |
| SPA | 1 (0.76) | 1 (0.76) | 2 (1.52) | 3 (2.86) | 2 (1.90) | 5 (4.76) | |
| Lymph node metastasis | | | | | | | <0.001 |
| Yes | 0 | 0 | 0 | 10 (9.52) | 4 (3.81) | 14 (13.33) | |
| No | 92 (69.70) | 40 (30.30) | 132 (100.00) | 63 (60.00) | 28 (26.67) | 91 (86.67) | |
| Maximum diameter | 7.20 ± 4.30 | 8.63 ± 5.12 | 7.63 ± 4.59 | 14.34 ± 5.82 | 15.19 ± 6.42 | 14.60 ± 5.99 | <0.001 |
| Lesion location | | | | | | | 0.923 |
| Right upper lobe | 34 (25.76) | 12 (9.09) | 46 (34.85) | 24 (22.86) | 12 (11.43) | 36 (34.29) | |
| Right middle lobe | 6 (4.55) | 0 | 6 (4.55) | 1 (0.95) | 2 (1.90) | 3 (2.86) | |
| Right lower lobe | 20 (15.15) | 11 (8.33) | 31 (23.48) | 16 (15.24) | 7 (6.67) | 23 (21.90) | |
| Left upper lobe | 23 (17.42) | 9 (6.82) | 32 (24.24) | 17 (16.19) | 9 (8.57) | 26 (24.76) | |
| Left lower lobe | 9 (6.82) | 8 (6.06) | 17 (12.88) | 15 (14.29) | 2 (1.90) | 17 (16.19) | |
| Density | | | | | | | <0.001 |
| pGGO | 51 (38.64) | 21 (15.91) | 72 (54.55) | 8 (7.62) | 1 (0.95) | 9 (8.57) | |
| mGGO | 36 (27.27) | 15 (11.36) | 51 (38.64) | 38 (36.19) | 20 (19.05) | 58 (55.24) | |
| SN | 5 (3.79) | 4 (3.03) | 9 (6.82) | 27 (25.71) | 11 (10.48) | 38 (36.19) | |
| Shape | | | | | | | <0.001 |
| Round | 70 (53.03) | 30 (22.73) | 100 (75.76) | 30 (28.57) | 10 (9.52) | 40 (38.10) | |
| Irregular | 22 (16.67) | 10 (7.58) | 32 (24.24) | 43 (40.95) | 22 (20.95) | 65 (61.90) | |
| Tumor-lung interface | | | | | | | 0.239 |
| Clear | 47 (35.61) | 19 (14.39) | 66 (50.00) | 44 (41.90) | 17 (16.19) | 61 (58.10) | |
| Unclear | 45 (34.09) | 21 (15.91) | 66 (50.00) | 29 (27.62) | 15 (14.29) | 44 (41.90) | |
| Lobulation | | | | | | | <0.001 |
| Yes | 58 (43.94) | 26 (19.70) | 84 (63.64) | 69 (65.71) | 30 (28.57) | 99 (94.29) | |
| No | 34 (25.76) | 14 (10.61) | 48 (36.36) | 4 (3.81) | 2 (1.90) | 6 (5.71) | |
| Spiculation | | | | | | | <0.001 |
| Yes | 35 (26.52) | 14 (10.61) | 49 (37.12) | 56 (53.33) | 26 (24.76) | 82 (78.10) | |
| No | 57 (43.18) | 26 (19.70) | 83 (62.88) | 17 (16.19) | 6 (5.71) | 23 (21.90) | |
| Bubblelike lucency | | | | | | | 0.418 |
| Yes | 35 (26.52) | 16 (12.12) | 51 (38.64) | 22 (20.95) | 13 (12.38) | 35 (33.33) | |
| No | 57 (43.18) | 24 (18.18) | 81 (61.36) | 51 (48.57) | 19 (18.10) | 70 (66.67) | |
| Air bronchogram | | | | | | | <0.001 |
| Yes | 33 (25.00) | 13 (9.85) | 46 (34.85) | 54 (51.43) | 23 (21.90) | 77 (73.33) | |
| No | 59 (44.70) | 27 (20.45) | 86 (65.15) | 19 (18.10) | 9 (8.57) | 28 (26.67) | |
| Vascular sign | | | | | | | <0.001 |
| Yes | 72 (54.55) | 33 (25.00) | 105 (79.55) | 72 (68.57) | 30 (28.57) | 102 (97.14) | |
| No | 20 (15.15) | 7 (5.30) | 27 (20.45) | 1 (0.95) | 2 (1.90) | 3 (2.86) | |
| Pleural traction | | | | | | | <0.001 |
| Yes | 32 (24.24) | 11 (8.33) | 43 (32.58) | 48 (45.71) | 20 (19.05) | 68 (64.76) | |
| No | 60 (45.45) | 29 (21.97) | 89 (67.42) | 25 (23.81) | 12 (11.43) | 37 (35.24) | |

pGGO, pure ground-glass opacity; mGGO, mixed ground-glass opacity; SN, solid nodule; AAH, atypical adenomatous hyperplasia; AIS, adenocarcinoma in situ; MIA, minimally invasive adenocarcinoma; IAC, invasive adenocarcinoma; LPA, lepidic-predominant adenocarcinoma; APA, acinar-predominant adenocarcinoma; PPA, papillary-predominant adenocarcinoma; MPA, micropapillary-predominant adenocarcinoma; SPA, solid-predominant adenocarcinoma.

TABLE 5 | ROC curve of the main factors affecting the Ki-67 expression level.

| Characteristics | AUC | B | S.E. | Wals | Exp(B) | Exp(B) | | P |
|----------------------|-------|--------|-------|-------|--------|-----------|----------|-------|
| | | | | | | Low limit | Up limit | |
| Pathological subtype | 0.809 | -1.459 | 0.519 | 7.90 | 0.232 | 0.084 | 0.643 | 0.005 |
| Air bronchogram sign | 0.711 | -0.813 | 0.406 | 4.014 | 0.444 | 0.200 | 0.982 | 0.045 |

AUC, area under curve; S.E., standard error; Exp, exponential function.



-HHL_glcm_MCC ($p < 0.001$), wavelet-LHH_glcm_MCC ($p < 0.001$), and wavelet-LLL_firstorder_Median ($p < 0.001$).

agreement with the actual probability in the training cohort (Figures 6C,D).

Development and Validation of the Radiomic Prediction Model

In the training set, the expression level of Ki-67 was taken as the dependent variable, and the CT radiomic features of lung adenocarcinoma were used as the independent variable to establish a pre-operative prediction model of Ki-67 expression level. The AUC value was 0.871 in the training dataset, the sensitivity was 76.7%, and the specificity was 83.7%, with a positive predictive value of 0.789. For the testing set, the classifier had an AUC value of 0.8, the sensitivity was 68.8%, and the specificity was 80%, with a positive predictive value of 0.733 (Table 7, Figures 6A,B). The calibration curve of the radiomic features also showed that the predicted probability was in good

DISCUSSION

Ki-67 is considered to represent the proliferative state of tumors and is a prognostic biomarker in multiple malignant tumors, such as breast, prostate, and lung cancer (14). Ki-67 has a broad prospect in the study of lung cancer, especially the occurrence, development, early diagnosis, and prognosis of ground-glass opacity (GGO) in early lung cancer under low-dose CT scans (25, 26). Ki-67 has been widely introduced into clinical practice to differentiate lung cancer subtypes and predict oncology outcomes (26–28). In our study, we systematically evaluated the expression level of Ki-67 according to the histological subtypes of lung adenocarcinoma and revealed the prognostic role of

TABLE 6 | Analysis of the radiomic features between negative and positive Ki-67 levels in the training set.

| Radiomic features | Ki-67 negative expression group (n = 92) | Ki-67 positive expression group (n = 73) | p |
|---|--|--|--------|
| | Mean (range) | Mean (range) | |
| lbp-3D-k_glrIm_LongRunHighGrayLevelEmphasis | -0.3747 (-2.55, 1.88) | 0.4722 (-0.89, 5.79) | <0.001 |
| lbp-3D-k_glrIm_ShortRunLowGrayLevelEmphasis | 0.3820 (-1.68, 6.27) | -0.4814 (-0.3279, -2.36) | <0.001 |
| log-sigma-3-0-mm-3D_gldm_GrayLevelVariance | -5.124 (-1.27, 1.40) | 0.6458 (-1.17, 2.80) | <0.001 |
| original_gldm_LowGrayLevelEmphasis | 0.1915 (-0.70, 7.08) | -0.2414 (-0.71, 3.68) | 0.004 |
| original_glrIm_LowGrayLevelRunEmphasis | 0.2163 (-0.78, 4.82) | -0.2726 (-0.80, 3.80) | 0.001 |
| wavelet-HHL_glcM_MCC | 0.2603 (-2.16, 3.68) | -0.3280 (-1.70, 1.57) | <0.001 |
| wavelet-LHH_glcM_MCC | 0.2364 (-1.52, 4.38) | -0.2980 (-2.01, 3.53) | 0.001 |
| wavelet-LLL_firstorder_Median | -0.4528 (-1.13, 2.01) | 0.5707 (-1.11, 2.30) | <0.001 |

MCC, Maximal Correlation Coefficient.

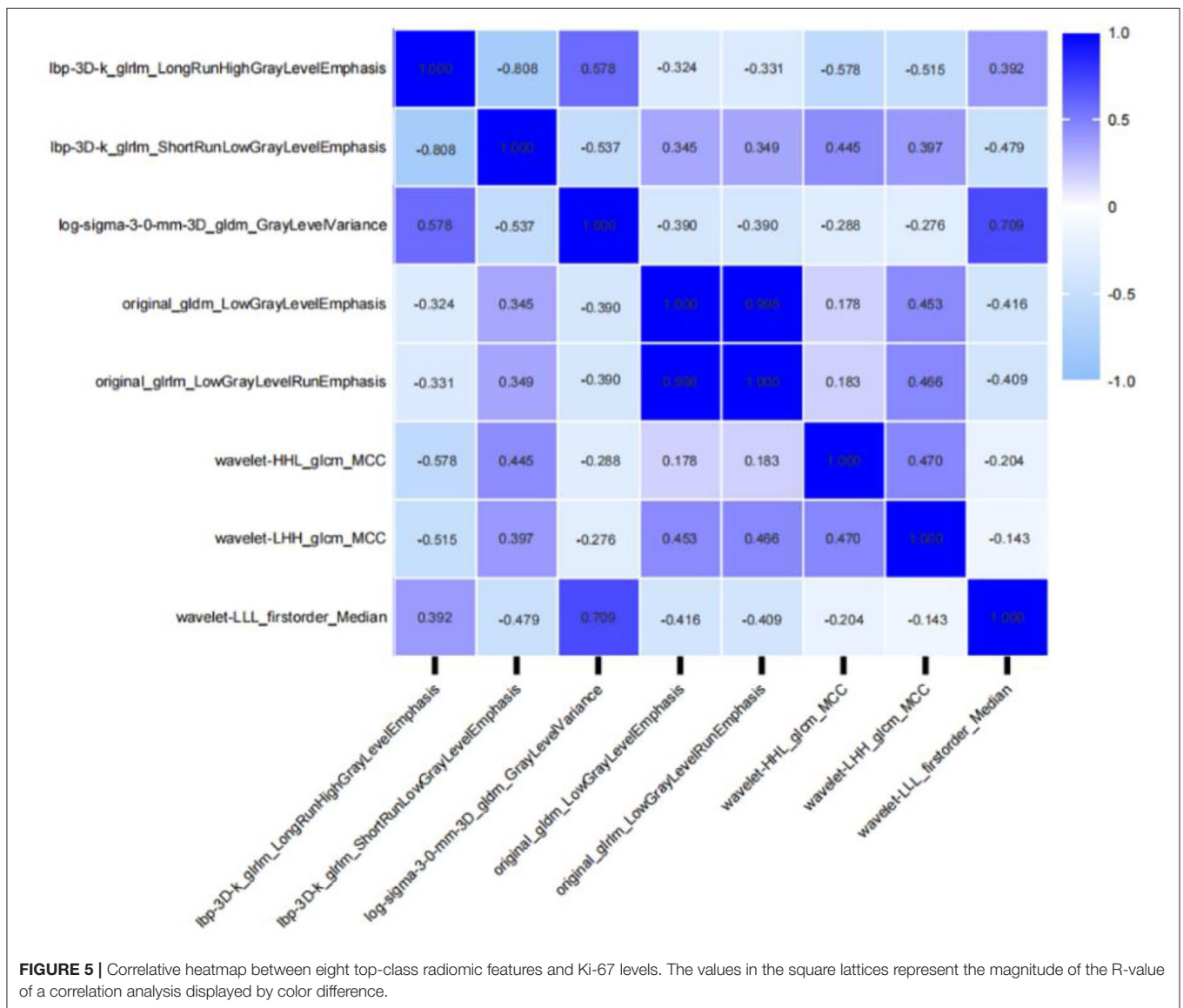


TABLE 7 | The predictive performance of radiomic classifier in training and validation sets.

| Datasets | AUC | SEN | SPE | Accuracy | PPV | NPV |
|------------------------|-------|-------|-------|----------|-------|-------|
| Training ($n = 165$) | 0.871 | 0.767 | 0.837 | 0.806 | 0.789 | 0.819 |
| Testing ($n = 72$) | 0.800 | 0.688 | 0.800 | 0.750 | 0.733 | 0.762 |

AUC, area under curve; SEN, sensitivity; SPE, specificity; PPV, positive predictive value; NPV, negative predictive value.

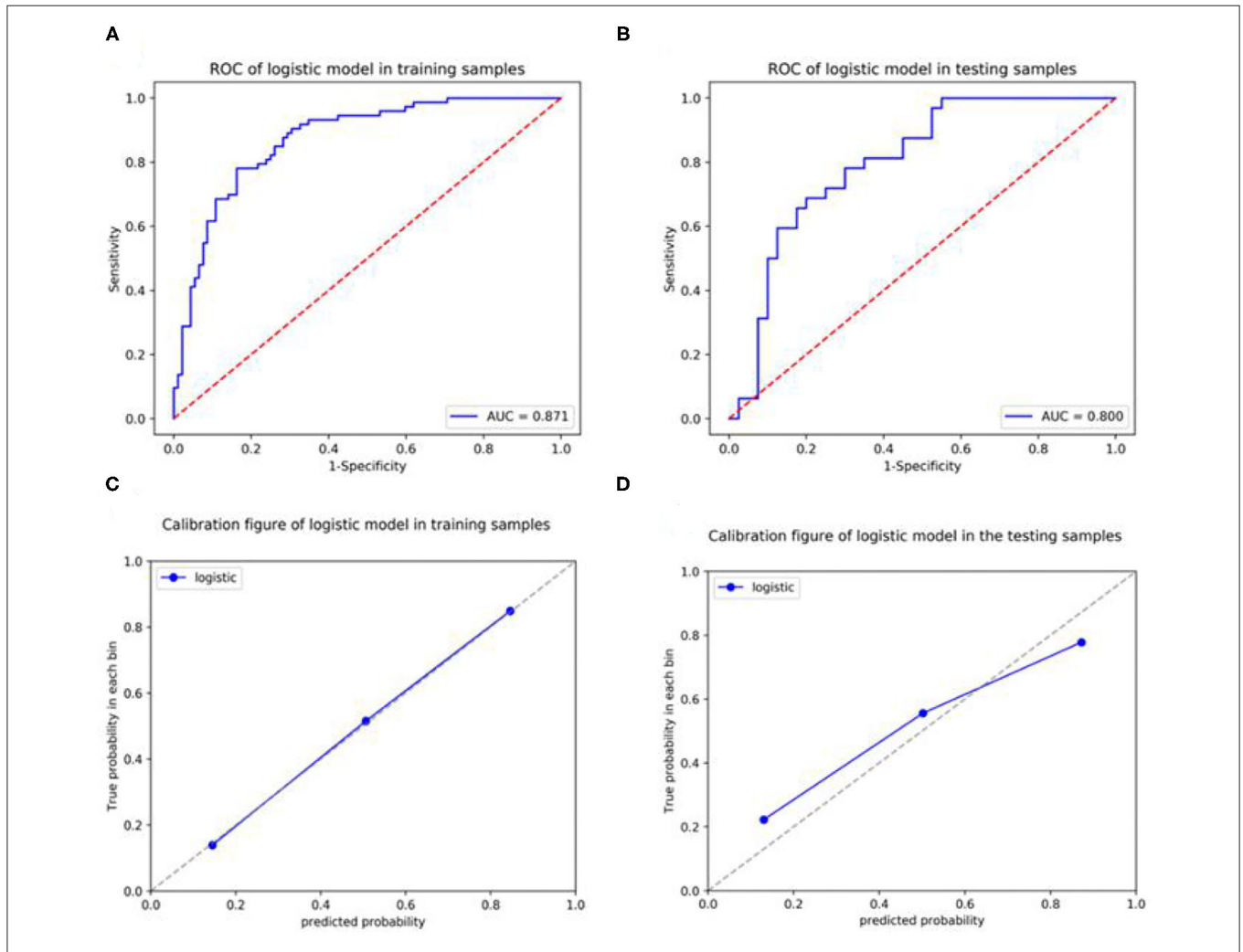


FIGURE 6 | Receiver operating curves (ROCs) and a calibration curve analysis for the radiomic signature for predicting the expression level of Ki-67 in the training set and testing set. [(A,C) training dataset, (B,D) testing dataset]. Calibration curves depict the calibration of each model in terms of the agreement between the predicted and actual probability of the positive Ki-67 expression level rate. The Y-axis represents the actual rate. The X-axis represents the predicted probability. The diagonal dotted line represents perfect prediction by an ideal model. The blue line represents the performance of the radiomic prediction model, of which a closer fit to the diagonal blue dotted line represents a better prediction.

Ki-67 in lung adenocarcinoma. Strikingly, we found that Ki-67 expression differed across lung adenocarcinoma histological subtypes, with IAC harboring the highest expression level, followed by the MIA, AIS, and AAH subtypes, which was consistent with the finding by Ishida et al. and Yan et al. (29, 30). Ki-67 expression levels demonstrated good performance in our study, with AUCs of 0.851, 0.787, and 0.872 for differentiating between MIA and IAC, AAH/AIS and MIA/IAC, and AAH/AIS/MIA and IAC, respectively. The Youden index

of the paired groups of pathological subtypes were 5.5, 6.5, and 5.5, respectively. It showed that the Ki-67 values were below 5% for non-invasive adenocarcinomas (AAH/AIS/MIA) and more than 5% for invasive adenocarcinomas. Notably, it means that Ki-67 expression could be identified as an independent prognostic factor of lung adenocarcinoma (28). The overexpression of Ki-67 infers poor differentiation and prognosis. Hence, the accurate pre-operative evaluation of the Ki-67 level may be helpful in distinguishing the different subtypes of patients with

lung adenocarcinoma (31). For some suspicious patients with follow-up observations and no indication of surgery or needle biopsy, Ki-67 could serve as a useful predictive biomarker to select suspicious lesions with high proliferation. The early detection of this cancer could enhance the cure of the disease and even prolong overall survival.

Several previous studies demonstrated that conventional CT images could be a non-invasive measurement to predict the Ki-67 index in lung adenocarcinoma. Our results showed that the degree of Ki-67 expression was related to nodule diameter, density, spiculation, lobulation, and air bronchogram sign. Moreover, an air bronchogram was the independent factor influencing the Ki-67 expression level, and the AUC in the ROC analysis for distinguishing different Ki-67 expression levels was 0.711. It inferred that the CT images of lung adenocarcinoma were related to the expression of Ki-67 (30). Our results were consistent with previous findings (32–36). Thus, the conventional CT examination might indirectly reflect the proliferative activity of lung adenocarcinoma, which was of high value to the early identification of the positive Ki-67 expression from negative Ki-67 expression and the facilitation of early diagnoses and individualized treatments, improving the survival rate. However, the ability of CT images to predict the Ki-67 index is controversial. Conventional CT provides limited information regarding lung adenocarcinoma grading and cannot replace the biopsy and surgery in obtaining specimens for a definitive diagnosis (37).

Radiomics can extract information-rich imaging functions with high throughput, which is different from traditional subjective imaging, and can quantify imaging information that the human eye cannot detect (15, 38, 39). In mathematics, radiomic features have different functions and definitions. Thus, it has a very good advantage in measuring the heterogeneity of tumor texture features (40). Several studies have shown that radiomics have been effective in predicting the Ki-67 index in multiple tumors (41). In this study, we established a pre-operative Ki-67 classification model in patients with lung adenocarcinoma using CT-based radiomic features. The result shows that eight radiomic features were significantly different between the negative Ki-67 group and the positive Ki-67 group ($p < 0.001$) (42). The CT-based radiomic predictive model demonstrated a stable and reliable performance, reaching an AUC of 0.871 and 0.8 and an accuracy of 80.6 and 75% in the training and testing cohorts, respectively. Therefore, the analysis revealed that CT-based radiomic features could pre-operatively predict Ki-67 levels in patients with lung adenocarcinoma, especially for suspicious patients under conservative treatment or patients who have lost the opportunity of a biopsy. The preliminary judgment of tumor proliferative activity through radiomic features can improve the accuracy and effectiveness of treatment, and could avoid the delay of disease and economic loss caused by ineffective treatment, which could have potential

implications for future patient management and aid in the implementation of precision medicine.

Choosing an appropriate Ki-67 cut-off value is convenient for clinicians to treat and manage patients. However, no consensus on the prognostic value of the Ki-67 expression level was found among the published studies, neither according to disease stage nor histological subtype. In previous studies on lung cancer, the cutoff values for Ki-67 prediction of prognosis were mostly used at 25, 30, 40, and 50% (43–45). For stage I lung adenocarcinoma, a cut-off value of 0.1 was commonly used. Ishida suggested that the Ki-67 index of 2.8% might be used as a marker to distinguish between MIA and AIS (29). Determining a cut-off value is often based on the median value. In this study, 5% was selected as the classification threshold based on our data characteristics and previous similar studies, and relatively good results were obtained, which indicated that proliferative activity with a Ki-67 expression level of 5% may be a crucial turning point for progression from non-invasive adenocarcinomas (AAH/AIS/MIA) to invasive adenocarcinomas.

Our study had some limitations. First, this study had a small sample size, which may increase concerns regarding selection bias. Moreover, this study was a single-centered retrospective study. Further studies involving multiple centers and a large number of patients are necessary. Second, the manual outline of ROIs is time and labor-consuming, and there is no standardized outline process and rules, which may lead to poor consistency among different radiologists. The automatic recognition of tumor lesions and the characterization of ROIs for feature extraction are some of the future research directions. Third, the largest diameter of the lung adenocarcinoma lesions included in this study was <3 cm, and there is a bias in the selection of study subjects, which may affect the results of the study. In the future, how to better mine information to assist clinical decision-making so that patients can get more accurate individualized treatments is also an opportunity and challenge in the development of radiomics.

In conclusion, Ki-67 expression levels with a cut-off value of 5% could be used to differentiate non-invasive lung adenocarcinomas (AAH/AIS/MIA) from invasive lung adenocarcinomas. The radiomic characteristics of CT have potential as non-invasive biomarkers for predicting Ki-67 levels in patients with lung adenocarcinoma, which might allow for a precise evaluation of tumor biological behavior, aid in clinical treatment decision making for the precise management of patients with lung adenocarcinoma, as well as provide supplemental information for depicting the heterogeneity of lung adenocarcinoma in different histological subtypes.

DATA AVAILABILITY STATEMENT

The original contributions presented in the study are included in the article/supplementary material, further inquiries can be directed to the corresponding author/s.

ETHICS STATEMENT

Written informed consent was obtained from the individual(s) for the publication of any potentially identifiable images or data included in this article.

AUTHOR CONTRIBUTIONS

ZH and ZX: conception and designation. ML and ZH: data collection. ML and ZA: data analysis and drafting the manuscript. ML and ZX: statistical analysis. YC and YL: technical support.

REFERENCES

- Allemani C, Matsuda T, Di Carlo V, Harewood R, Matz M, Nikšić M, et al. Global surveillance of trends in cancer survival 2000-14 (CONCORD-3): analysis of individual records for 37 513 025 patients diagnosed with one of 18 cancers from 322 population-based registries in 71 countries. *Lancet*. (2018) 391:1023–75. doi: 10.1016/S0140-6736(17)33326-3
- Travis WD, Brambilla E, Noguchi M, Nicholson AG, Geisinger KR, Yatabe Y, et al. International association for the study of lung cancer/american thoracic society/european respiratory society international multidisciplinary classification of lung adenocarcinoma. *J Thorac Oncol*. (2011) 6:244–85. doi: 10.1097/JTO.0b013e318206a221
- Jamal-Hanjani M, Quezada SA, Larkin J, Swanton C. Translational implications of tumor heterogeneity. *Clin Cancer Res*. (2015) 21:1258–66. doi: 10.1158/1078-0432.CCR-14-1429
- Weissferdt A, Kalhor N, Marom EM, Benveniste MF, Godoy MC, Correa AM, et al. Early-stage pulmonary adenocarcinoma (T1N0M0): a clinical, radiological, surgical, and pathological correlation of 104 cases. The MD Anderson Cancer Center Experience. *Mod Pathol*. (2013) 26:1065–75. doi: 10.1038/modpathol.2013.33
- Zhou Y, Hu W, Chen P, Abe M, Shi L, Tan SY, et al. Ki67 is a biological marker of malignant risk of gastrointestinal stromal tumors: a systematic review and meta-analysis. *Medicine*. (2017) 96:e7911. doi: 10.1097/MD.0000000000007911
- Pyo JS, Kim NY. Meta-analysis of prognostic role of Ki-67 labeling index in gastric carcinoma. *Int J Biol Markers*. (2017) 32:e447–53. doi: 10.5301/ijbm.5000277
- Chen M, Li X, Wei Y, Qi L, Sun YS. Spectral CT imaging parameters and Ki-67 labeling index in lung adenocarcinoma. *Chin J Cancer Res*. (2020) 32:96–104. doi: 10.21147/j.issn.1000-9604.2020.01.11
- Wei DM, Chen WJ, Meng RM, Zhao N, Zhang XY, Liao DY, et al. Augmented expression of Ki-67 is correlated with clinicopathological characteristics and prognosis for lung cancer patients: an up-dated systematic review and meta-analysis with 108 studies and 14,732 patients. *Respir Res*. (2018) 19:150. doi: 10.1186/s12931-018-0843-7
- Okudela K, Woo T, Saigusa Y, Arai H, Matsumura M, Mitsui H, et al. A method to obtain reproducible Ki-67 indices in lung adenocarcinoma. *Histopathology*. (2021) 78:414–23. doi: 10.1111/his.14234
- Yamashita S, Moroga T, Tokuishi K, Miyawaki M, Chujo M, Yamamoto S, et al. Ki-67 labeling index is associated with recurrence after segmentectomy under video-assisted thoracoscopic surgery in stage I non-small cell lung cancer. *Ann Thorac Cardiovasc Surg*. (2011) 17:341–6. doi: 10.5761/atcs.0a.10.01573
- Sterlacci W, Stockinger R, Schmid T, Bodner J, Hilbe W, Waldthaler C, et al. The elderly patient with surgically resected non-small cell lung cancer—a distinct situation? *Exp Gerontol*. (2012) 47:237–42. doi: 10.1016/j.exger.2011.12.008
- Gu Q, Feng Z, Liang Q, Li M, Deng J, Ma M, et al. Machine learning-based radiomics strategy for prediction of cell proliferation in non-small cell lung cancer. *Eur J Radiol*. (2019) 118:32–7. doi: 10.1016/j.ejrad.2019.06.025
- Polk SL, Choi JW, McGettigan MJ, Rose T, Ahmed A, Kim J, et al. Multiphase computed tomography radiomics of pancreatic intraductal papillary mucinous neoplasms to predict malignancy. *World J Gastroenterol*. (2020) 26:3458–71. doi: 10.3748/wjg.v26.i24.3458
- Boros M, Moncea D, Moldovan C, Podoleanu C, Georgescu R, Stolnicu S. Intratumoral heterogeneity for Ki-67 index in invasive breast carcinoma: a study on 131 consecutive cases. *Appl Immunohistochem Mol Morphol*. (2017) 25:338–40. doi: 10.1097/PAL.0000000000000315
- Gillies RJ, Kinahan PE, Hricak H. Radiomics: images are more than pictures, they are data. *Radiology*. (2016) 278:563–77. doi: 10.1148/radiol.2015151169
- Limkin EJ, Sun R, Dercle L, Zacharaki EI, Robert C, Reuzé S, et al. Promises and challenges for the implementation of computational medical imaging (radiomics) in oncology. *Ann Oncol*. (2017) 28:1191–206. doi: 10.1093/annonc/mdx034
- Yu H, Meng X, Chen H, Liu J, Gao W, Du L, et al. Predicting the level of tumor-infiltrating lymphocytes in patients with breast cancer: usefulness of mammographic radiomics features. *Front Oncol*. (2021) 11:628577. doi: 10.3389/fonc.2021.628577
- Avanzo M, Stancanello J, El Naqa I. Beyond imaging: the promise of radiomics. *Phys Med*. (2017) 38:122–39. doi: 10.1016/j.ejmp.2017.05.071
- Lee G, Lee HY, Park H, Schiebler ML, van Beek EJR, Ohno Y, et al. Radiomics and its emerging role in lung cancer research, imaging biomarkers and clinical management: state of the art. *Eur J Radiol*. (2017) 86:297–307. doi: 10.1016/j.ejrad.2016.09.005
- Wilson R, Devaraj A. Radiomics of pulmonary nodules and lung cancer. *Transl Lung Cancer Res*. (2017) 6:86–91. doi: 10.21037/tlcr.2017.01.04
- Zhou B, Xu J, Tian Y, Yuan S, Li X. Correlation between radiomic features based on contrast-enhanced computed tomography images and Ki-67 proliferation index in lung cancer: a preliminary study. *Thorac Cancer*. (2018) 9:1235–40. doi: 10.1111/1759-7714.12821
- Hyun-Ju Lee, Young Tae Kim, Chang Hyun Kang, Zhao B, Tan Y, Lawrence H. Schwartz, et al. Epidermal growth factor receptor mutation in lung adenocarcinomas: relationship with CT characteristics and histologic subtypes. *Radiology*. (2013) 268:254–64. doi: 10.1148/radiol.13112553
- Travis WD, Brambilla E, Nicholson AG, Yatabe Y, Austin JHM, Beasley MB, et al. The 2015 World Health Organization classification of lung tumors: impact of genetic, clinical and radiologic advances since the 2004 classification. *J Thorac Oncol*. (2015) 10:1243–60. doi: 10.1097/JTO.0000000000000630
- K.T.Dermawan J, Farver CF. The role of histologic grading and Ki-67 index in predicting outcomes in pulmonary carcinoid tumors. *Am J Surg Pathol*. (2019) 44:224–31. doi: 10.1097/PAS.0000000000001358
- van Bree SH, Nemethova A, Cailotto C, Gomez-Pinilla PJ, Matteoli G, Boeckstaens GE. New therapeutic strategies for postoperative ileus. *Nat Rev Gastroenterol Hepatol*. (2012) 9:675–83. doi: 10.1038/nrgastro.2012.134
- Wen S, Zhou W, Li CM, Hu J, Hu XM, Chen P, et al. Ki-67 as a prognostic marker in early-stage non-small cell lung cancer in Asian patients: a meta-analysis of published studies involving 32 studies. *BMC Cancer*. (2015) 15:520. doi: 10.1186/s12885-015-1524-2

All authors contributed to the article and approved the submitted version.

FUNDING

This research was supported by grants from the National Natural Science Foundation of China (No. 82171931), Natural Science Foundation of Guangdong (No. 2015A030313753), the Science and Technology Program of Guangzhou (Nos. 201903010032 and 202102080572), and the Panyu Science and Technology Program of Guangzhou (Nos. 2017-Z04-12, 2019-Z04-01, and 2019-Z04-23).

27. Borghaei H, Paz-Ares L, Horn L, Spigel DR, Steins M, Ready NE, et al. Nivolumab vs. docetaxel in advanced nonsquamous non-small-cell lung cancer. *N Engl J Med.* (2015) 373:1627–39. doi: 10.1056/NEJMoa1507643
28. Li Z, Li F, Pan C, He Z, Pan X, Zhu Q, et al. Tumor cell proliferation (Ki-67) expression and its prognostic significance in histological subtypes of lung adenocarcinoma. *Lung Cancer.* (2021) 154:69–75. doi: 10.1016/j.lungcan.2021.02.009
29. Ishida H, Shimizu Y, Sakaguchi H, Nitanda H, Kaneko K, Yamazaki N, et al. Distinctive clinicopathological features of adenocarcinoma *in situ* and minimally invasive adenocarcinoma of the lung: a retrospective study. *Lung Cancer.* (2019) 129:16–21. doi: 10.1016/j.lungcan.2018.12.020
30. Yan J, Wang H, Zhou H, He H, Qiu L, Wang Z. Correlation between expression of Ki-67 and MSCT signs in different types of lung adenocarcinoma. *Medicine.* (2020) 99:e18678. doi: 10.1097/MD.00000000000018678
31. Warth A, Cortis J, Soltermann A, Meister M, Budczies J, Stenzinger A, et al. Tumour cell proliferation (Ki-67) in non-small cell lung cancer: a critical reappraisal of its prognostic role. *Br J Cancer.* (2014) 111:1222–9. doi: 10.1038/bjc.2014.402
32. Si MJ, Tao XF, Du GY, Cai LL, Han HX, Liang XZ, et al. Thin-section computed tomography-histopathologic comparisons of pulmonary focal interstitial fibrosis, atypical adenomatous hyperplasia, adenocarcinoma *in situ*, and minimally invasive adenocarcinoma with pure ground-glass opacity. *Eur J Radiol.* (2016) 85:1708–15. doi: 10.1016/j.ejrad.2016.07.012
33. Moon Y, Sung SW, Lee KY, Sim SB, Park JK. Pure ground-glass opacity on chest computed tomography: predictive factors for invasive adenocarcinoma. *J Thorac Dis.* (2016) 8:1561–70. doi: 10.21037/jtd.2016.06.34
34. Jin X, Zhao SH, Gao J, Wang DJ, Wu J, Wu CC, et al. CT characteristics and pathological implications of early stage (T1N0M0) lung adenocarcinoma with pure ground-glass opacity. *Eur Radiol.* (2015) 25:2532–40. doi: 10.1007/s00330-015-3637-z
35. Takahashi M, Shigematsu Y, Ohta M, Tokumasu H, Matsukura T, Hirai T. Tumor invasiveness as defined by the newly proposed IASLC/ATS/ERS classification has prognostic significance for pathologic stage IA lung adenocarcinoma and can be predicted by radiologic parameters. *J Thorac Cardiovasc Surg.* (2014) 147:54–9. doi: 10.1016/j.jtcvs.2013.08.058
36. Lim HJ, Ahn S, Lee KS, Han J, Shim YM, Woo S, et al. Persistent pure ground-glass opacity lung nodules \geq 10 mm in diameter at CT scan: histopathologic comparisons and prognostic implications. *Chest.* (2013) 144:1291–9. doi: 10.1378/chest.12-2987
37. Tamrazi B, Pekmezci M, Aboian M, Tihan T, Glastonbury CM. Apparent diffusion coefficient and pituitary macroadenomas: pre-operative assessment of tumor atypia. *Pituitary.* (2017) 20:195–200. doi: 10.1007/s11102-016-0759-5
38. Zhang N, Zeng Q, Chen C, Yu J, Zhang X. Distribution, diagnosis, and treatment of pulmonary sequestration: report of 208 cases. *J Pediatr Surg.* (2019) 54:1286–92. doi: 10.1016/j.jpedsurg.2018.08.054
39. Ahmed AA, Elmohr MM, Fuentes D, Habra MA, Fisher SB, Perrier ND, et al. Radiomic mapping model for prediction of Ki-67 expression in adrenocortical carcinoma. *Clin Radiol.* (2020) 75:479.e17–22. doi: 10.1016/j.crad.2020.01.012
40. Davnall F, Yip CS, Ljungqvist G, Selmi M, Ng F, Sanghera B, et al. Assessment of tumor heterogeneity: an emerging imaging tool for clinical practice? *Insights Imaging.* (2012) 3:573–89. doi: 10.1007/s13244-012-0196-6
41. Fan Y, Chai Y, Li K, Fang H, Mou A, Feng S, et al. Non-invasive and real-time proliferative activity estimation based on a quantitative radiomics approach for patients with acromegaly: a multicenter study. *J Endocrinol Invest.* (2020) 43:755–65. doi: 10.1007/s40618-019-01159-7
42. Guo J, Ren J, Shen J, Cheng R, He Y. Do the combination of multiparametric MRI-based radiomics and selected blood inflammatory markers predict the grade and proliferation in glioma patients? *Diagn Interv Radiol.* (2021) 27:440–9. doi: 10.5152/dir.2021.20154
43. Jakobsen JN, Sørensen JB. Clinical impact of ki-67 labeling index in non-small cell lung cancer. *Lung Cancer.* (2013) 79:1–7. doi: 10.1016/j.lungcan.2012.10.008
44. Lin L, Cheng J, Tang D, Zhang Y, Zhang F, Xu J, et al. The associations among quantitative spectral CT parameters, Ki-67 expression levels and EGFR mutation status in NSCLC. *Sci Rep.* (2020) 10:3436. doi: 10.1038/s41598-020-60445-0
45. Ahn HK, Jung M, Ha SY, Lee JI, Park I, Kim YS, et al. Clinical significance of Ki-67 and p53 expression in curatively resected non-small cell lung cancer. *Tumour Biol.* (2014) 35:5735–40. doi: 10.1007/s13277-014-1760-0

Conflict of Interest: The authors declare that the research was conducted in the absence of any commercial or financial relationships that could be construed as a potential conflict of interest.

The reviewer ZW declared a shared affiliation with one of the authors, ML, to the handling editor at the time of the review.

Publisher's Note: All claims expressed in this article are solely those of the authors and do not necessarily represent those of their affiliated organizations, or those of the publisher, the editors and the reviewers. Any product that may be evaluated in this article, or claim that may be made by its manufacturer, is not guaranteed or endorsed by the publisher.

Copyright © 2021 Huang, Lyu, Ai, Chen, Liang and Xiang. This is an open-access article distributed under the terms of the Creative Commons Attribution License (CC BY). The use, distribution or reproduction in other forums is permitted, provided the original author(s) and the copyright owner(s) are credited and that the original publication in this journal is cited, in accordance with accepted academic practice. No use, distribution or reproduction is permitted which does not comply with these terms.